

J. Phys. (Paris) **25**, 704 (1964).

<sup>8</sup>E. F. Neuzil and R. H. Lindsay, Phys. Rev. **131**, 1697 (1963).

<sup>9</sup>Studies in penetration of charged particles in matter. Committee on Nuclear Science, Nuclear Science Series Report No. 39, National Academy of Sciences-National Research Council, Washington, D.C., 1964 (unpublished).

<sup>10</sup>The stopping-power parameter  $I$  for vanadium nitride is calculated as follows:

$$\log \langle I_{\text{VN}} \rangle = \frac{1}{\rho_{\text{VN}}} \left\langle \frac{A}{Z} \right\rangle_{\text{VN}} \left[ \frac{Z_{\text{N}} \rho_{\text{N}}}{A_{\text{N}}} \log I_{\text{N}} + \frac{Z_{\text{V}} \rho_{\text{V}}}{A_{\text{V}}} \log I_{\text{V}} \right].$$

$\rho_{\text{VN}}$  is the specific mass of the vanadium nitride used, and

$$\left\langle \frac{Z}{A} \right\rangle_{\text{VN}} = \frac{1}{\rho_{\text{VN}}} \left[ \frac{Z_{\text{N}} \rho_{\text{N}}}{A_{\text{N}}} + \frac{Z_{\text{V}} \rho_{\text{V}}}{A_{\text{V}}} \right].$$

$\rho_{\text{N}}$  and  $\rho_{\text{V}}$  are the partial densities of nitrogen and vanadium in the vanadium nitride. The mean atomic excitation energy  $I$  of nitrogen is known experimentally; for vanadium it has been calculated following a relation due to Sternheimer:  $I/Z = 9.76 + 58.8Z^{-1.48}$  eV. Finally, the value  $\langle I_{\text{VN}} \rangle = 200$  eV was obtained.

## Cross-Section and Polarization Measurements for the ${}^3\text{H}({}^3\text{He}, n){}^5\text{Li}$ Reaction\*

J. T. Klopčič† and S. E. Darden

University of Notre Dame, Notre Dame, Indiana 46556

(Received 8 February 1971)

Measurements of the angular distribution and polarization of neutrons from the reaction  ${}^3\text{H}({}^3\text{He}, n){}^5\text{Li}$  have been made for mean  ${}^3\text{He}$  bombarding energies of 2.70 and 3.55 MeV. Polarizations were measured using a  ${}^4\text{He}$  gas scintillator, and cross sections were determined using a liquid scintillator employing pulse-shape discrimination. Contributions from the three-body breakup channel  ${}^3\text{H}({}^3\text{He}, np){}^4\text{He}$  were removed by assuming these neutrons to be unpolarized and to have a statistical energy distribution in the high-energy portion of the neutron spectrum. The angular distribution of neutrons from the reaction  ${}^3\text{H}({}^3\text{He}, n){}^5\text{Li}$  exhibits a broad peak in the vicinity of  $\theta_{\text{c.m.}} = 45^\circ$ . The neutron polarization was found to be negative at all angles investigated, and reaches a minimum value of  $-0.30$  at  $\theta_{\text{c.m.}} = 125^\circ$ ,  $E_{3\text{He}} = 2.7$  MeV. Excitation functions for the cross section were measured at laboratory angles of  $0$  and  $40^\circ$  for  ${}^3\text{He}$  energies between 0.7 and 3.8 MeV. The reaction data can be reproduced qualitatively with a simple two-nucleon-transfer distorted-wave Born-approximation calculation, but the  ${}^3\text{He}$ - ${}^3\text{H}$  potential parameters used do not reproduce published elastic scattering data at somewhat higher energy.

### I. INTRODUCTION

Among the nuclear reactions involving very light nuclei, those in which the entrance channel consists of  ${}^3\text{He} + {}^3\text{H}$  have as yet not been studied very extensively; in particular, the  ${}^3\text{H}({}^3\text{He}, n){}^5\text{Li}$  reaction has received very little attention to date.<sup>1,2</sup> The study of this reaction is complicated by the fact that  ${}^5\text{Li}$  is unbound and the neutrons are emitted in the presence of neutrons from three-body breakup into  $\alpha + n + p$ . Using a proton recoil telescope, Barry, Batchelor, and Macefield (BBM)<sup>2</sup> observed the spectrum of neutrons produced by bombarding tritium with  ${}^3\text{He}$  consists of a prominent peak corresponding to neutrons from the two-body final state  ${}^5\text{Li} + n$  ( $Q = 10.13$  MeV), superimposed on a continuum of neutrons from the three-body final state  ${}^4\text{He} + n + p$  and from the breakup of unstable members of other two-body states. For a  ${}^3\text{He}$  bombarding energy of 3.2 MeV, the angular distribution of neutrons from  ${}^3\text{H}({}^3\text{He}, n){}^5\text{Li}$  was found to exhibit a broad peak near  $40^\circ$  (lab), some-

what suggestive of an  $l=1$  double stripping process involving transfer of two protons from  ${}^3\text{He}$  to  ${}^3\text{H}$ . The possibility of two-nucleon transfer from the triton to the  ${}^3\text{He}$  particle, which might also be expected to occur in this reaction, could not be excluded by the data of BBM.

Angular-distribution measurements on the mirror reaction  ${}^3\text{He}({}^3\text{H}, p){}^5\text{He}$  have been confined for the most part to bombarding energies below 1100 keV.<sup>3,4</sup> To the extent that Coulomb effects can be neglected, the angular distribution for this reaction should be the same as for  ${}^3\text{H}({}^3\text{He}, n){}^5\text{Li}$ . Kühn and Schlenk<sup>3</sup> observed the angular distribution in  ${}^3\text{He}({}^3\text{H}, p){}^5\text{He}$  to change smoothly from near-isotropy at a bombarding energy of 460 keV to distributions broadly peaked around  $80^\circ$  (c.m.) at a bombarding energy near 1100 keV.

It is of interest to see to what extent the  ${}^3\text{H}$ - ${}^3\text{He}$ ,  ${}^5\text{Li}$  and  ${}^3\text{He}$ ,  ${}^3\text{H}$ ,  ${}^5\text{He}$  reactions can be regarded as two-body reactions separate from other processes such as breakup into  ${}^4\text{He} + n + p$ . If, for example, the  ${}^3\text{H}({}^3\text{He}, n){}^5\text{Li}$  reaction should proceed

predominantly by  $L = 1$  transfer of two protons to  ${}^3\text{H}$ , one would expect the angular distribution to be peaked forward of  $90^\circ$ , and the polarization of the outgoing neutrons should be determined mainly by the spin-dependent potentials for the entrance and exit channels. Since little information regarding optical potentials for either entrance or exit channels exists and since the residual nucleus is unbound, a description of this reaction in terms of a simple two-nucleon transfer will, of course, be laden with uncertainty.

In the experiment reported here, cross sections and polarizations for the  ${}^3\text{H}({}^3\text{He}, n){}^5\text{Li}$  reaction have been measured at mean bombarding energies of 2.70 and 3.55 MeV, and excitation curves of cross section have been measured at lab angles of  $0$  and  $40^\circ$  for  ${}^3\text{He}$  energies between 0.7 and 3.6 MeV. A preliminary report on these measurements has already appeared in abstract form.<sup>5</sup>

## II. EXPERIMENTAL METHOD

### A. General

All measurements were carried out with the Notre Dame 4-MeV accelerator. The ion beams were momentum-analyzed and collimated before reaching the target. Tritium targets consisted of thin copper disks containing a layer of titanium into which tritium had been absorbed. For the cross-section measurements, the titanium was 270-keV thick to 3-MeV  ${}^3\text{He}^+$  ions. The target and a portion of the beam pipe served as a Faraday cage. A collimator at a potential of a few hundred volts served to suppress secondary electrons. Ion beam currents used for the cross-section measurements were of the order of  $0.1 \mu\text{A}$ .

The low efficiency of the double-scattering technique necessitated a much higher reaction rate for the polarization measurements. Since the reaction cross section is low ( $\approx 1 \text{ mb/sr}$ ) and beam currents could not exceed a few  $\mu\text{A}$  without causing excessive target deterioration, a relatively thick target (600 keV for 3-MeV  ${}^3\text{He}^+$  ions) was used for the polarization measurements. To avoid overheating the target, the beam current was limited to  $5 \mu\text{A}$ , the beam was defocussed and magnetically wobbled over a small ellipse ( $0.75 \text{ cm} \times 0.33 \text{ cm}$ ), and the target was water cooled.

### B. Cross-Section Measurements

Cross-section data were taken with a liquid scintillator (Ne213;  $5 \text{ cm} \times 5 \text{ cm}$  diam) employing pulse-shape discrimination to eliminate  $\gamma$  rays. Angular-distribution measurements were carried out with an angular resolution of  $3^\circ$  over an angular range extending from  $0$  to  $140^\circ$  in the c.m. sys-

tem. Pulses from proton recoils in the scintillator were stored in 256-channel pulse-height spectra. Extraction of the energy spectrum of neutrons incident on a recoil scintillator from the measured pulse-height spectrum required a knowledge of the recoil spectrum produced by monoenergetic neutrons. The shape of the monoenergetic neutron recoil spectrum was calculated using the  $n$ - $p$  scattering cross section and the detector size and shape, taking into account the effects of double-scattered neutrons and folding into the spectrum a Gaussian function to represent the finite resolution of the detector system. Effects of scattering from carbon nuclei and events in which neutrons were scattered more than twice in the scintillator were estimated and found to be negligible. By using the width of the Gaussian resolution func-

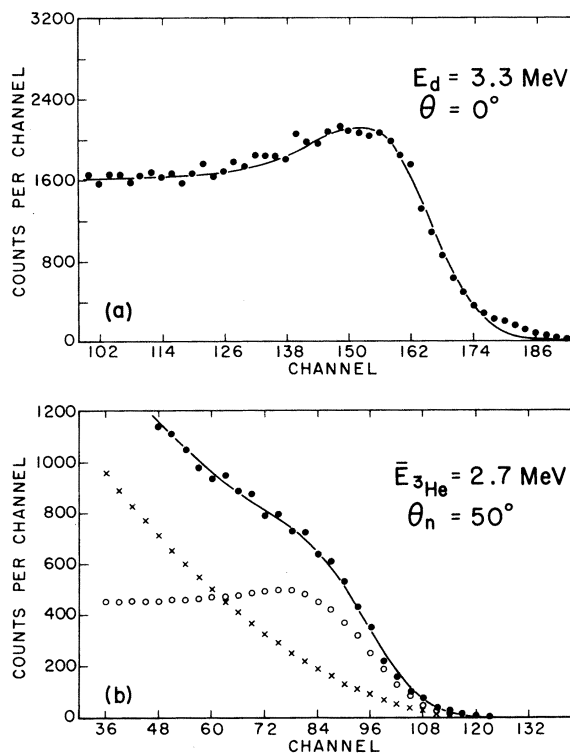


FIG. 1. Proton-recoil spectra in the liquid scintillator used for the cross-section measurements. (a) Monoenergetic-neutron-recoil spectrum produced by 18-MeV neutrons from the  ${}^3\text{H}(d,n)$  reaction. The solid curve is the calculated spectrum. Only the upper half of the spectrum is shown. (b) Recoil spectrum produced by neutrons from the  ${}^3\text{H}({}^3\text{He}, n)$  reaction. The solid curve is the calculated spectrum. The separate recoil spectra produced by  ${}^3\text{H}({}^3\text{He}, n){}^5\text{Li}$  neutrons and by  ${}^3\text{H}({}^3\text{He}, np){}^4\text{He}$  neutrons are illustrated by the circles and the  $\times$ 's, respectively. The width of the resolution function used to calculate the recoil spectrum of the  ${}^3\text{H}({}^3\text{He}, n){}^5\text{Li}$  neutrons was increased to take into account the width ( $\approx 1 \text{ MeV}$ ) of the ground state of  ${}^5\text{Li}$ .

tion as an adjustable parameter, measured spectra produced by monoenergetic neutrons from the  ${}^3\text{H}(d, n){}^4\text{He}$  and  ${}^9\text{Be}(\alpha, n){}^{12}\text{C}$  reactions could be well reproduced. Figure 1(a) shows the upper portion of the measured and calculated recoil spectrum for 18-MeV neutrons from the  ${}^3\text{H}(d, n){}^4\text{He}$  reaction. A resolution function having a full width at half maximum of 12% was required to reproduce the observed spectrum.

Recoil spectra produced by neutrons from  ${}^3\text{H}({}^3\text{He}, n)$  are complicated by the existence of a continuum of neutrons from the three-body final state. The energies of these neutrons extend from 0 to about 2 MeV above the  ${}^5\text{Li}$  peak. In the analysis the spectrum of three-body neutrons was assumed to be purely statistical.<sup>6</sup> The recoil spectrum resulting from three-body neutrons is a superposition of properly normalized monoenergetic-neutron-recoil spectra corresponding to each point of the continuous spectrum. The total recoil spectrum is a sum of the three-body-neutron-recoil spectrum and a monoenergetic-neutron-recoil spectrum corresponding to the  ${}^3\text{H}({}^3\text{He}, n){}^5\text{Li}$  neutrons. Figure 1(b) shows an example of a spectrum produced by  ${}^3\text{H}({}^3\text{He}, n)$  neutrons, together with the calculated spectrum. The presence of the neutron group from the  ${}^3\text{H}({}^3\text{He}, n){}^5\text{Li}$  reaction is apparent from the change in slope in the spectrum near channel 84. Parameters used in fitting the spectrum are an amplitude factor for the in-

tensity of the  ${}^5\text{Li}$  neutrons and a similar factor for the three-body-breakup neutrons. From the values of these parameters, cross sections for the  ${}^3\text{H}({}^3\text{He}, n){}^5\text{Li}$  and  ${}^3\text{H}({}^3\text{He}, np){}^4\text{He}$  reactions can be extracted. A noticeably poorer fit to the measured spectrum results if the relative magnitudes of the two amplitude factors are changed by 10%.

It was possible to assign absolute values to cross sections obtained from the recoil spectra by normalizing  ${}^3\text{H}(d, n){}^4\text{He}$  cross sections measured with the same target to published values.<sup>7</sup> As a check on the cross-section-analysis procedure, the angular dependence of the differential cross section for the  ${}^3\text{H}(d, n){}^4\text{He}$  reaction was measured for a deuteron bombarding energy of 3.0 MeV and found to be in excellent agreement with results of previous investigators.<sup>7</sup>

### C. Polarization Measurements

Elastic scattering by  ${}^4\text{He}$  was used as an analyzing reaction for the neutron-polarization measurements, which utilized the same general procedure used in a previous experiment at this laboratory.<sup>8</sup> The  ${}^4\text{He}$  was contained in a high-pressure scintillation cell that differed from conventional cells<sup>9</sup> in two respects. First, the active volume of the cell (4-cm diam; 6-cm length) was surrounded by a thin liquid-nitrogen cooling jacket. Designed to allow a more dense filling at a given pressure, it

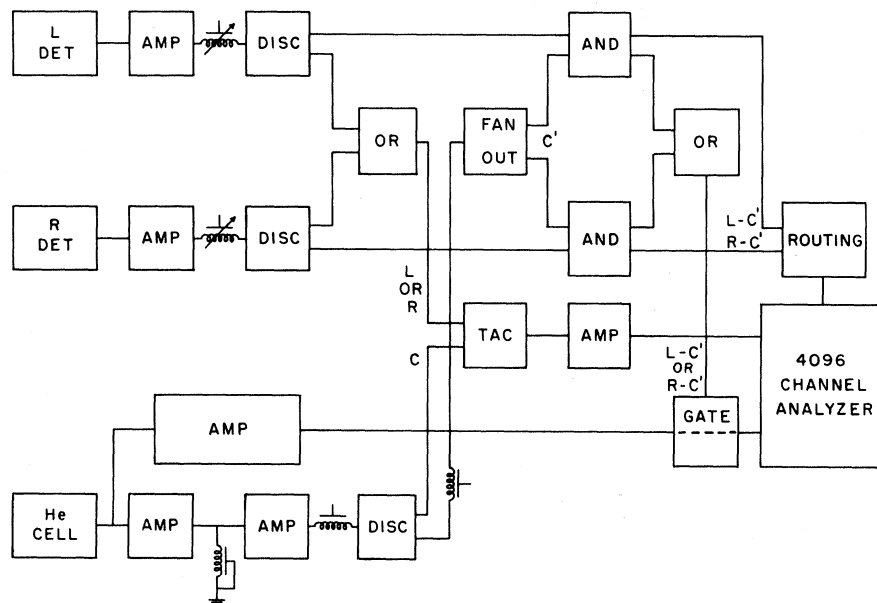


FIG. 2. Block diagram of the circuitry used for the polarization measurements. The output of the time-to-amplitude converter and the linear signal from the helium cell were stored in one of two  $32 \times 32$ -channel arrays selected by the routing circuit. The logic pulses are 20 nsec in width. In order for events to be stored, a coincidence was also required between a neutron detector pulse and the pulse from the He cell which had been delayed by 20 nsec. This insured that the He cell pulse preceded the neutron detector pulse and reduced the accidental background by a factor of 2.

proved more useful in practice for purifying the cell *in situ*. The second feature was the use of cylindrical geometry and the incorporation of a high-voltage center wire into the cell. It has been found<sup>10</sup> that a high electric field in a low-pressure scintillation cell produces amplification of the light produced by a recoiling charged particle in the cell, somewhat like the charge amplification in a proportional counter. An attempt was made to observe this phenomenon in a high-pressure cell, with a view towards development of a high-light-output high-resolution cell. Light amplification was observed, but cell resolution was not improved. Since the present study did not warrant further work on the cell development, the cell was used in the conventional manner. However, it does appear that a high-light-output high-resolution cell could be built using high field amplification.

The He cell was operated at a filling of 180 atm. with a mixture of 95%  $^4\text{He}$  and 5% Xe. Cell resolution with a polonium  $\alpha$  source mounted on the center wire was  $12\frac{1}{2}\%$ . The gas scintillator, paraffin and W-Ni shielding, and two neutron detectors were mounted on a movable table which could

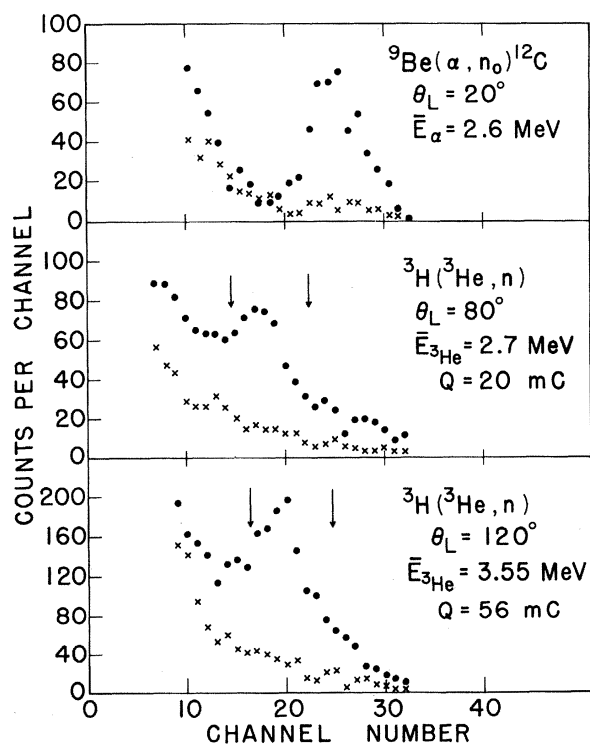


FIG. 3. Examples of coincidence recoil spectra produced by neutrons from  $^9\text{Be}(\alpha, n_0)^{12}\text{C}$  and  $^3\text{H}(^3\text{He}, n)^5\text{Li}$ . The spectra shown correspond to coincidences occurring in a 5-nsec-wide time interval. Accidental coincidences are indicated by the  $\times$ 's. The arrows shown on the  $^3\text{H}(^3\text{He}, n)$  spectra indicate the portion of the recoil peak used in calculating asymmetries.

be pivoted about the position of the tritium target. Rectangular plastic scintillators  $5\text{ cm} \times 7.5\text{ cm} \times 15\text{ cm}$  were used as neutron detectors with the largest dimension vertical and the largest face towards the He cell. The neutron detectors were positioned 40 cm from the He cell at a mean scattering angle of  $123^\circ$  (lab).

Recoil  $^4\text{He}$ -ion pulses in the gas scintillator were detected in coincidence with the corresponding neutron pulses from the neutron detectors. The circuitry used (Fig. 2) was similar to that employed in previous experiments at this laboratory.<sup>8, 11</sup> Each neutron-detector-gas-scintillator coincidence event was stored in one of two 32-channel  $\times$  32-channel two-dimensional arrays. One axis of the two-parameter spectrum corresponded to  $\alpha$ -recoil energy in the gas scintillator, while the other corresponded to the time between the occurrence of the  $\alpha$ -recoil pulse and the neutron detector pulse. Energy calibration was provided by Po- $\alpha$  spectra as well as by spectra taken with monoenergetic neutrons from the  $^3\text{H}(d, n)^4\text{He}$  and  $^9\text{Be}(\alpha, n)^{12}\text{C}$  reactions. The time axis was calibrated with monoenergetic-neutron spectra and with the use of known delays in the logic circuitry. Figure 3 shows representative  $\alpha$ -recoil energy spectra obtained by projecting 5-nsec-wide portions of the two-parameter spectra onto the recoil-energy axis. In each case shown, the time interval over which counts have been summed was centered on the appropriate value corresponding to the neutron group of interest. Accidental coincidences were obtained for each measurement by summing the counts over an identical time interval displaced along the time axis by 10 nsec. Typically, the accidental background amounted to 15% or less of the counts in the  $\alpha$ -recoil peak. The effect of three-body-breakup neutrons is clearly evident in the spectra produced by neutrons from the  $^3\text{H}(^3\text{He}, n)$  reaction. In obtaining numbers of counts

TABLE I. Polarization test measurements.

$\theta_{\text{lab}}$	$^9\text{Be}(\alpha, n)^{12}\text{C}$ $E_\alpha = 2.6\text{ MeV}$		
	$P_n(\theta)$ This work	Ref. 11	Ref. 12
0	$-0.005 \pm 0.02$		
20	$0.11 \pm 0.04$	$0.16 \pm 0.03$	
40	$0.52 \pm 0.06$	$0.40 \pm 0.09$	$0.49 \pm 0.04$
60	$0.46 \pm 0.06$	$0.37 \pm 0.03$	$0.6 \pm 0.1$
80	$0.27 \pm 0.05$	$0.10 \pm 0.03$	
90	$0.05 \pm 0.05$	$0.10 \pm 0.02$	
	$^3\text{H}(d, n)^4\text{He}$ $E_d = 3.3\text{ MeV}$ Ref. 13		
60	$-0.25 \pm 0.09$	$-0.203 \pm 0.02$	
70	$-0.23 \pm 0.04$	$-0.233 \pm 0.02$	

to be used in computing asymmetries, the portion of the recoil peak between the limits indicated by the arrows in Fig. 3 was used. No attempt was made to correct the asymmetry data for background from room-scattered neutrons or double scattering in the He cell, as these effects are expected to be small compared to other uncertainties in the polarization measurements.

In a typical asymmetry-measurement sequence, the two sets of coincidence data would be stored in two quadrants of a 4096-channel analyzer. The table with cell, shielding, and neutron detectors would then be rotated to a position corresponding to the same reaction angle on the opposite side of the beam tube and spectra would be taken in the remaining two quadrants of the analyzer memory. Some of the asymmetry data were also taken by interchanging the two neutron detectors. The asymmetry-measurement procedures involving both rotation of the table and interchange of the neutron detectors were checked by measuring the polarization of neutrons from the  ${}^9\text{Be}(\alpha, n){}^{12}\text{C}$  and  ${}^3\text{H}(d, n){}^4\text{He}$  reactions. The results of these measurements (Table I) are in satisfactory agreement with values obtained by previous investigators.<sup>11-13</sup>

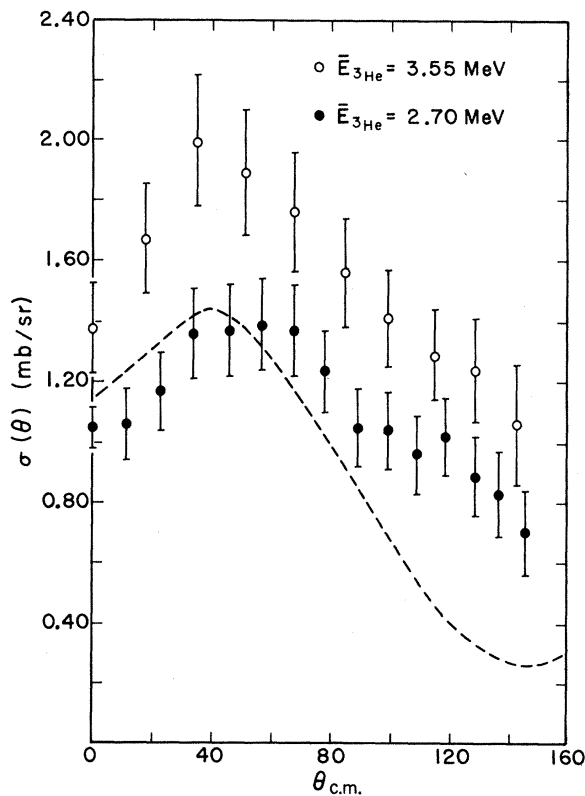


FIG. 4. Angular distributions of neutrons from the  ${}^3\text{H}({}^3\text{He}, n){}^5\text{Li}$  reaction for mean  ${}^3\text{He}$  bombarding energies of 3.55 and 2.70 MeV. The cross sections are given in the c.m. system. The dashed curve is discussed in the text.

### III. RESULTS

Results of the angular-distribution measurements for neutrons from the  ${}^3\text{H}({}^3\text{He}, n){}^5\text{Li}$  reaction are shown in Fig. 4 as a function of c.m. reaction angle. The laboratory and c.m. cross sections are given in Table II. In Fig. 5 are shown the results of the excitation functions of the cross-section measured for  $\theta_{\text{lab}} = 0$  and  $40^\circ$ . Estimated uncertainties in the cross sections, which are generally of the order of 10%, arise from approximately equal contributions from statistical uncertainties in the data and from uncertainty in the separation of the monoenergetic-neutron-recoil spectrum from the measured spectrum. The absolute uncertainty associated with the normalization of the cross section appears to be about 5% or less.<sup>7</sup> Also given in Table II are cross-section values for production of neutrons in the three-body final state. The fifth column of the table contains  $d^2\sigma/d\Omega dE_n$ , the differential cross section per unit energy for three-body neutrons having the same energy as neutrons from the  ${}^3\text{H}({}^3\text{He}, n){}^5\text{Li}$  reaction. In the last column are given differential cross sections for three-body neutrons of all energies. These cross sections must be considered very approximate, since they have been obtained

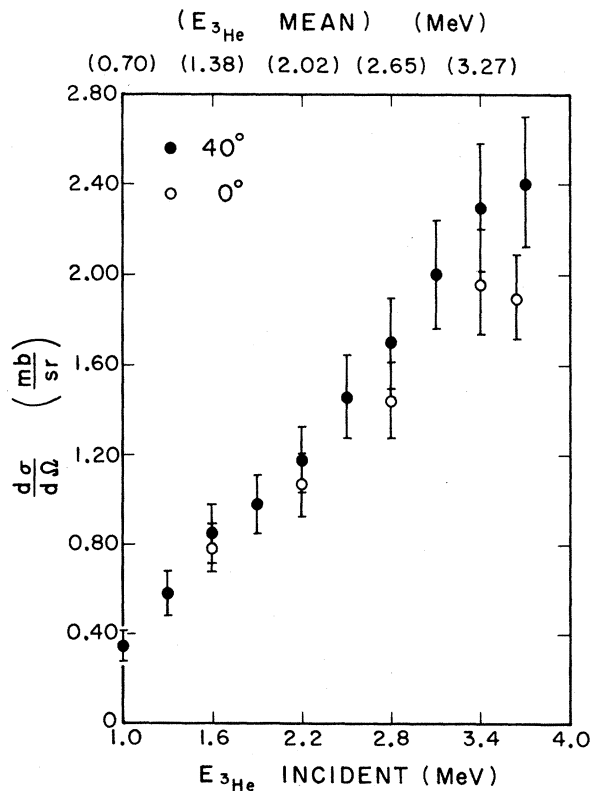


FIG. 5. Excitation function of laboratory cross sections for  ${}^3\text{H}({}^3\text{He}, n){}^5\text{Li}$  for laboratory angles of  $0$  and  $40^\circ$ .

TABLE II. Laboratory and c.m. cross sections.

$\theta_{\text{lab}}$	${}^3\text{H}({}^3\text{He}, n){}^5\text{Li}$		$d\sigma/d\Omega$ c.m., (mb/sr)	${}^3\text{H}({}^3\text{He}, np){}^4\text{He}$	
	$d\sigma/d\Omega$ lab (mb/sr)	$\theta_{\text{c.m.}}$		$d^2\sigma/d\Omega dE$ (mb/sr MeV)	$d\sigma/d\Omega$ (mb/sr)
$\bar{E}_{{}^3\text{He}} = 2.7 \text{ MeV}$					
0	1.4 ± 0.10	0.0	1.05 ± 0.07	0.059 ± 0.021	0.51 ± 0.18
10	1.4 ± 0.15	11.5	1.06 ± 0.12	0.058 ± 0.021	0.50 ± 0.18
20	1.53 ± 0.16	23.0	1.17 ± 0.13	0.054 ± 0.019	0.46 ± 0.16
30	1.74 ± 0.19	34.4	1.36 ± 0.15	0.051 ± 0.018	0.43 ± 0.15
40	1.70 ± 0.19	45.6	1.37 ± 0.15	0.048 ± 0.017	0.39 ± 0.14
50	1.67 ± 0.19	56.7	1.39 ± 0.15	0.051 ± 0.018	0.39 ± 0.14
60	1.54 ± 0.16	67.6	1.37 ± 0.15	0.048 ± 0.017	0.35 ± 0.13
70	1.36 ± 0.15	78.2	1.24 ± 0.13	0.049 ± 0.018	0.34 ± 0.13
80	1.09 ± 0.14	88.6	1.05 ± 0.13	0.047 ± 0.018	0.32 ± 0.13
90	1.03 ± 0.13	98.6	1.04 ± 0.13	0.048 ± 0.018	0.32 ± 0.13
100	0.90 ± 0.12	108.6	0.96 ± 0.13	0.055 ± 0.020	0.34 ± 0.13
110	0.90 ± 0.12	118.2	1.02 ± 0.13	0.051 ± 0.020	0.32 ± 0.13
120	0.75 ± 0.11	127.6	0.89 ± 0.13	0.057 ± 0.022	0.32 ± 0.14
130	0.67 ± 0.11	136.7	0.83 ± 0.14	0.063 ± 0.025	0.34 ± 0.14
140	0.54 ± 0.11	145.6	0.70 ± 0.14	0.060 ± 0.025	0.30 ± 0.14
$\bar{E}_{{}^3\text{He}} = 3.55 \text{ MeV}$					
0	1.89 ± 0.21	0.0	1.38 ± 0.15	0.064 ± 0.022	0.57 ± 0.20
15	2.27 ± 0.25	17.5	1.67 ± 0.19	0.059 ± 0.021	0.52 ± 0.18
30	2.60 ± 0.29	34.9	1.98 ± 0.22	0.053 ± 0.019	0.45 ± 0.16
45	2.36 ± 0.26	46.3	1.89 ± 0.21	0.051 ± 0.018	0.42 ± 0.15
60	2.05 ± 0.23	68.5	1.76 ± 0.20	0.051 ± 0.018	0.39 ± 0.14
75	1.68 ± 0.19	84.5	1.56 ± 0.18	0.046 ± 0.018	0.36 ± 0.13
90	1.39 ± 0.15	100.0	1.41 ± 0.16	0.051 ± 0.018	0.34 ± 0.13
105	1.16 ± 0.14	114.5	1.29 ± 0.15	0.050 ± 0.018	0.33 ± 0.14
120	1.02 ± 0.14	128.5	1.24 ± 0.17	0.060 ± 0.024	0.35 ± 0.15
135	0.81 ± 0.16	141.9	1.06 ± 0.20	0.065 ± 0.026	0.36 ± 0.16

from the observed three-body neutron portion of the recoil spectra assuming the shape of the three-body-neutron spectrum to be given by phase-space considerations alone.<sup>6</sup> The values of  $d^2\sigma/d\Omega dE_n$  are more reliable, since in obtaining these cross sections it was only necessary to assume that the high-energy portion of the three-body-neutron spectrum has a statistical shape. That this assumption is at least approximately valid is evidenced by the agreement between measured and calculated recoil spectra [Fig. 1(b)].

#### Polarizations

Results of the polarization measurements are given in Table III. The third column gives the polarization of all neutrons from the  ${}^3\text{H}({}^3\text{He}, n)$  reaction having energy within an interval bounded by the energies  $E_0(1 \pm 0.15)$ , where  $E_0$  is the neutron energy corresponding to the center of the  ${}^3\text{H}({}^3\text{He}, n)$ - ${}^5\text{Li}$  peak. The values of  $P_n$  were obtained from asymmetries calculated using the recoil peak counts in the two-parameter spectra, corrected for accidental coincidences. In calculating the neutron polarizations from measured asymmetries,

the appropriately averaged analyzing power of helium as determined from the phase shifts of Morgan<sup>14</sup> was used. If the three body neutrons are assumed to be unpolarized, the polarization of neutrons leaving  ${}^5\text{Li}$  in its ground state is given by

$$P_n({}^5\text{Li}) = P_n \left[ 1 + \left( \frac{d^2\sigma}{d\Omega dE} \right)_{\text{three body}} \frac{\Delta E}{\left( \frac{d\sigma}{d\Omega} \right)_{{}^5\text{Li}}} \right], \quad (1)$$

where  $\Delta E$  denotes the width of the energy interval over which counts are summed in the two-parameter recoil spectrum, and  $(d^2\sigma/d\Omega dE)_{\text{three body}}$  has been averaged over this energy interval. Values of  $P_n({}^5\text{Li})$  obtained in this way are given in the fourth column of Table III, and are plotted versus c.m. reaction angle in Fig. 6. The uncertainties indicated for the polarization measurements arise almost entirely from statistical uncertainties in the number of counts. In the last column of Table III are the values of the polarization for all neutrons having energies corresponding to  ${}^5\text{Li}$  being left in its first excited state ( $E_x \approx 3.8 \text{ MeV}$ ). These polarizations were extracted from the data in the appropriate portion of the two-parameter spectra.

TABLE III. Results of the polarization measurements. The Basel convention is followed throughout.

$\theta_{\text{lab}}$	$\theta_{\text{c.m.}}$	$P_n$	$P_n(^6\text{Li})$	$P_n(^5\text{Li}^*)$
$\bar{E}_{^3\text{He}} = 2.7 \text{ MeV}$				
10	11.5	$-0.012 \pm 0.046$	$-0.013 \pm 0.046$	$-0.005 \pm 0.052$
20	23.0	$-0.073 \pm 0.031$	$-0.079 \pm 0.034$	$0.041 \pm 0.048$
30	34.4	$-0.125 \pm 0.025$	$-0.134 \pm 0.027$	$-0.040 \pm 0.070$
40	45.6	$-0.081 \pm 0.025$	$-0.084 \pm 0.026$	$0.000 \pm 0.082$
45	51.2	$-0.094 \pm 0.030$	$-0.100 \pm 0.032$	$-0.005 \pm 0.042$
50	56.7	$-0.093 \pm 0.049$	$-0.099 \pm 0.052$	$0.016 \pm 0.067$
60	67.6	$-0.099 \pm 0.031$	$-0.106 \pm 0.033$	$0.004 \pm 0.047$
70	78.3	$-0.134 \pm 0.062$	$-0.147 \pm 0.068$	$0.066 \pm 0.049$
80	88.7	$-0.098 \pm 0.031$	$-0.106 \pm 0.033$	$0.066 \pm 0.037$
90	98.8	$-0.158 \pm 0.036$	$-0.174 \pm 0.040$	$0.072 \pm 0.047$
100	108.7	$-0.182 \pm 0.029$	$-0.204 \pm 0.034$	$0.067 \pm 0.042$
110	118.3	$-0.253 \pm 0.032$	$-0.286 \pm 0.038$	$0.062 \pm 0.043$
120	127.6	$-0.262 \pm 0.031$	$-0.296 \pm 0.038$	$0.080 \pm 0.039$
130	136.7	$-0.200 \pm 0.040$	$-0.227 \pm 0.045$	$0.128 \pm 0.044$
$\bar{E}_{^3\text{He}} = 3.5 \text{ MeV}$				
20	23.4	$-0.105 \pm 0.044$	$-0.112 \pm 0.047$	$0.051 \pm 0.061$
30	34.9	$-0.109 \pm 0.036$	$-0.115 \pm 0.038$	$0.006 \pm 0.059$
45	51.9	$-0.088 \pm 0.028$	$-0.093 \pm 0.030$	$0.033 \pm 0.051$
60	68.5	$-0.058 \pm 0.029$	$-0.062 \pm 0.031$	
75	84.5	$-0.085 \pm 0.028$	$-0.090 \pm 0.030$	$0.083 \pm 0.048$
90	99.8	$-0.118 \pm 0.035$	$-0.127 \pm 0.038$	$0.140 \pm 0.058$
105	114.5	$-0.207 \pm 0.028$	$-0.223 \pm 0.030$	$0.071 \pm 0.046$
120	128.5	$-0.149 \pm 0.029$	$-0.165 \pm 0.032$	$0.113 \pm 0.045$

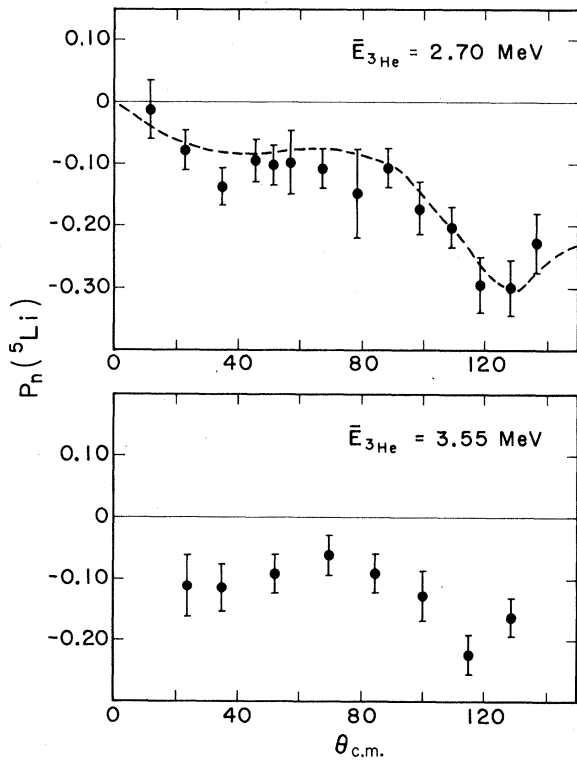


FIG. 6. Polarization of neutrons from the  $^3\text{H}(^3\text{He}, n)^5\text{Li}$  reaction as a function of c.m. reaction angle. The dashed curve is discussed in the text.

#### IV. DISCUSSION

Results of the angular-distribution measurements for  $^3\text{H}(^3\text{He}, n)^5\text{Li}$  presented here are in qualitative agreement with the results of Barry *et al.*<sup>2</sup> The agreement is good at forward and backward angles but our cross sections are about 20% lower in the vicinity of the peak near  $40^\circ$  than those of Ref. 2. Unpublished angular-distribution measurements by Hollandsworth<sup>15</sup> obtained using time-of-flight techniques for a  $^3\text{He}$  energy of 3 MeV agree well in shape with the present results. The data of Kühn and Schlenk<sup>3</sup> on the mirror reaction  $^3\text{He}(^3\text{H}, p)^5\text{He}$ , when transposed to the laboratory system, agree within assigned errors with the excitation-curve data of Fig. 5. The total cross section for the  $\alpha + n + p$  decay channel obtained from the data in the last column of Table II is approximately 4.5 mb. This result is very approximate, owing to the uncertainty in the shape of the three-body-breakup-neutron spectrum. To the extent that the assumption of a statistical spectrum shape is correct this number represents the cross section only for direct breakup into  $\alpha + n + p$ . This follows from the fact that the measured value of  $(d\sigma/d\Omega)_{\text{three body}}$  is determined primarily by the upper portion of the neutron energy spectrum, which contains no contribution from the decay channels  $\alpha + d^* \rightarrow \alpha + n + p$  and  $^5\text{He} + p \rightarrow \alpha + n + p$ , and relative-

TABLE IV. Potential parameters used in the DWBA calculation for the  ${}^3\text{H}({}^3\text{He}, n){}^5\text{Li}$  reaction.

	$V_0$ (MeV)	$r_0$ (F)	$a$ (F)	$W_S$ (MeV)	$r_0$ (F)	$a$ (F)	$V_{so}$ (MeV)	$r_0$ (F)	$a$ (F)
${}^3\text{He} + {}^3\text{H}$	140	1.2	0.6	10	1.2	0.6	5	1.2	0.6
$n - {}^5\text{Li}$	42	1.4	0.25	8	1.4	0.6	16	1.0	0.25

ly little contribution from the  ${}^5\text{Li}^* + n'$  decay channel. Comparison of this three-body-breakup cross section with the results of other investigators is difficult, since most of the values obtained from measurements on charged-particle spectra also involve assumptions as to the shape of the energy spectrum or the angular distribution of the emitted particles. Kühn and Schlenk<sup>3</sup> give a value of  $29.5 \pm 3.3$  mb for the breakup cross section at 1100 keV, but this number appears to include all channels except  $\alpha + d$  and  ${}^5\text{He} + p$ . On the basis of their neutron spectrum, which extends over most of the neutron energy range, BBM<sup>2</sup> obtain a value of  $20 \pm 4$  mb for the cross section of all reactions leading to neutron emission excepting  ${}^3\text{H}({}^3\text{He}, n){}^5\text{Li}$ . Their conclusion that the cross section for  ${}^3\text{H}({}^3\text{He}, n){}^5\text{Li}$  is an order of magnitude larger than that for  ${}^3\text{He}({}^3\text{H}, p){}^5\text{He}$  seems unwarranted in view of the agreement between our data and those of Kühn and Schlenk at 1100 keV. Smith, Jarmie, and Lockett<sup>4</sup> also obtained comparable values for the  ${}^3\text{H}({}^3\text{He}, n){}^5\text{Li}$  and  ${}^3\text{He}({}^3\text{H}, p){}^5\text{He}$  cross sections on the basis of their analysis of proton and  $\alpha$  spectra observed at 30 and 90° when  ${}^3\text{He}$  was bombarded with 1.9-MeV tritons. These authors obtained a differential cross section (assumed isotropic) of 2.4 mb/sr for the uncorrelated-breakup channel. This value exceeds our result for the breakup cross section by a factor of 6, but it is also based on their fit to the entire charged-particle spectrum.

In addition to statistical uncertainties, there is probably some systematic uncertainty in the polarization data associated with the magnitude of the contribution of the three-body-breakup neutrons. This uncertainty is difficult to estimate without accurate knowledge of the shape of the neutron spectrum, but it is probably comparable with the uncertainties indicated in Fig. 6.

The general appearance of the  ${}^3\text{H}({}^3\text{He}, n){}^5\text{Li}$  angular distribution data are suggestive of a two-nucleon forward stripping mechanism for the reaction. Any attempt to apply a simple distorted-wave Born-approximation (DWBA) two-nucleon stripping calculation to this reaction encounters a number of obstacles. For one thing, elastic scattering data for the entrance channel from which optical potentials can be obtained are not available

for bombarding energies below 5 MeV<sup>16,17</sup> and such data are unobtainable for the exit channel. The fact that the odd proton in  ${}^5\text{Li}$  is unbound is an additional complicating factor in any calculation. Also, there is no obvious reason why the reaction should proceed by the transfer of two protons from  ${}^3\text{He}$  to  ${}^3\text{H}$  in preference to the transfer of a proton and a neutron from  ${}^3\text{H}$  to  ${}^3\text{He}$ . Finally, it is not clear that the  ${}^3\text{H}({}^3\text{He}, n){}^5\text{Li}$  reaction can be treated separately from the three-body-breakup process and other decay modes which end up as  $\alpha + n + p$ . While recognizing these limitations on the applicability of the simple two-nucleon stripping model, an attempt was made to reproduce the cross-section and polarization data assuming the reaction to proceed by  $L = 1$  transfer of the two protons of  ${}^3\text{He}$  to  ${}^3\text{H}$ . In carrying out the calculation,<sup>18</sup> the proton transferred into a  $p_{3/2}$  state was assumed to be bound by 50 keV. The results appear to be insensitive to the details of the wave function for the  $p_{3/2}$  proton, presumably owing to the tight binding of the proton transferred to the  $s_{1/2}$  state. A realistic set of parameters (Table IV) was found which reproduce the general shape of the cross-section and polarization data, as shown by the dashed curves in Figs. 4 and 6. The calculated cross section in Fig. 4 has been multiplied by a factor of 1.15. However, these parameters do not reproduce the  ${}^3\text{He} + {}^3\text{H}$  elastic scattering data at higher energies. The principal change required to approximately fit the scattering data at 5.8 MeV<sup>17</sup> is a reduction in the depth of the real potential from 140 to 88 MeV, but this change completely destroys the agreement with the reaction data. It is, of course, possible that a strongly energy-dependent potential would be required to reproduce the  ${}^3\text{He} - {}^3\text{H}$  elastic scattering data between 3 and 6 MeV, but without having data for the lower energy it is difficult to conclude very much about the  ${}^3\text{He} - {}^3\text{H}$  optical potentials. However, from the results of the DWBA calculation, it appears possible that the  ${}^3\text{H}({}^3\text{He}, n){}^5\text{Li}$  reaction can be understood in terms of a two-nucleon stripping model. More definite conclusions must await additional  ${}^3\text{H} + {}^3\text{He}$  elastic scattering data and a calculation which takes into account properly both of the stripping modes referred to above.

## V. ACKNOWLEDGMENTS

The authors would like to acknowledge the effort of Albert Betz in the early phases of this work, and to thank Professor P. D. Kunz for providing the computer program DWUCK. We also wish to express our thanks to Professor Paul R. Chagnon for advice regarding the electronics of the polarization measurements.

\*Work supported in part by the National Science Foundation.

†NASA Fellow, present address: Nuclear Effects Laboratory, Edgewood Arsenal, Maryland 21010

<sup>1</sup>L. Youn, G. Osentinsii, N. Sodnom, A. Govorov, I. Sizov, and V. Salatskii, *Zh. Eksperim. i Teor. Fiz.* **39**, 225 (1960) [transl.: *Soviet Phys. - JEPT* **12**, 163 (1961)].

<sup>2</sup>J. Barry, R. Batchelor, and B. Macefield, in *Proceedings of the Rutherford Jubilee Conference, Manchester, 1961*, edited by J. Birks (Heywood and Company, Ltd., London, England, 1962).

<sup>3</sup>B. Kühn and B. Schlenk, *Nucl. Phys.* **48**, 353 (1963).

<sup>4</sup>D. Smith, N. Jarmie, and A. Lockett, *Phys. Rev.* **129**, 495 (1963).

<sup>5</sup>T. Klopcic and S. E. Darden, in *Proceedings of the Third International Polarization Symposium*, edited by H. H. Barshall and W. Haeberli (University of Wisconsin Press, Madison, Wisconsin).

<sup>6</sup>G. Ohlsen, *Nucl. Instr. Methods* **37**, 240 (1965).

<sup>7</sup>S. Bame and J. Perry, *Phys. Rev.* **107**, 1616 (1957).

<sup>8</sup>A. F. Behof, J. M. Hevezi, and G. Spalek, *Nucl. Phys.* **84**, 290 (1966).

<sup>9</sup>R. Shamu, *Nucl. Instr. Methods* **14**, 297 (1961).

<sup>10</sup>C. Conde and A. Policarpo, *Nucl. Instr. Methods* **53**, 7 (1967).

<sup>11</sup>G. Lietz, S. Trevino, A. Behof, and S. E. Darden, *Nucl. Phys.* **67**, 193 (1965).

<sup>12</sup>T. R. Donoghue, private communication.

<sup>13</sup>W. Büsse, J. Christiansen, D. Hilscher, U. Morfeld, J. Scheer, and W. Schröder, *Nucl. Phys.* **A100**, 490 (1967).

<sup>14</sup>G. Morgan, Ph.D. thesis, Duke University, 1967 (unpublished).

<sup>15</sup>C. Hollandsworth, private communication.

<sup>16</sup>M. Ivanovich, P. Young, and G. Ohlsen, *Nucl. Phys.* **A110**, 441 (1968).

<sup>17</sup>A. Bacher, R. Spiger, and T. Tombrello, *Nucl. Phys.* **A119**, 481 (1968).

<sup>18</sup>Fortran-IV computer code and instructions written by P. D. Kunz, unpublished.

Muon Capture in  $\text{Li}^6$  in the Ditrion Channel\*

B. R. Wienke and S. L. Meyer

*Department of Physics, Northwestern University, Evanston, Illinois 60201*

(Received 19 October 1971)

Within the context of the impulse approximation we analyze the reaction  $\mu^- + \text{Li}^6 \rightarrow \text{H}^3 + \text{H}^3 + \nu$  using the current-current theory of weak interactions and an  $\alpha$ - $d$  model of  $\text{Li}^6$  fitted to the binding energy and charge radius of  $\text{Li}^6$ . The model is tested by considering the channel  $\mu^- + \text{Li}^6 \rightarrow \text{He}^6 + \nu$ . Within the limitations of our stated approximations, total rates are estimated for these two modes and the combined triton distribution given for the ditriton channel.

## I. INTRODUCTION

We hope to exhibit some of the pertinent details of the capture process

$$\mu^- + \text{Li}^6 \rightarrow \text{H}^3 + \text{H}^3 + \nu \quad (1.1)$$

which is a channel interesting in connection with a proposed experiment to measure the muon neutrino mass.<sup>1</sup> Discussion of the experimental aspects of muon capture in the above channel will be reserved for another communication. We present the analysis in a general form to facilitate its application to any of the remaining channels.

Theoretical studies of muon-capture processes in lithium are numerous,<sup>2</sup> though we are unaware of any consideration of the ditriton final state. Basically, an impulse approximation, in which the capture is effected on a single proton, has been coupled to weak-interaction theory to describe muon-capture processes. Recourse is made in this paper to these techniques using cluster models of the relevant nuclei for which pertinent momentum structures are exhibited. More particularly, an  $\alpha$ - $d$  model of  $\text{Li}^6$  is assumed in which trial wave functions have been fitted to the lithium binding energy and charge radius using variational